Mechanism of low-frequency Raman scattering from the acoustic vibrations of dielectric nanoparticles

M. Mattarelli,[*] M. Montagna, and F. Rossi

Dipartimento di Fisica, CSMFO group, Università di Trento, Via Sommarive 14, I-38050 Trento, Italy

A. Chiasera and M. Ferrari

IFN-CNR, Istituto di Fotonica e Nanotecnologie, CSMFO group, Via Sommarive 14, I-38050 Trento, Italy

The depolarization ratio of the quadrupolar vibrations and the relative intensity of the symmetric $l=0$ and quadrupolar $l=2$ acoustic vibrations in the Raman spectra of some dielectric nanocrystals has been calculated. A dipole-induced-dipole model can account for the depolarized spectra from quadrupolar vibrations, but cannot be at the origin of the polarized peak from the symmetric vibration. Bond polarizability seems to be the main physical mechanism at the origin of Raman scattering from these modes. The study indicates that the quadrupolar modes or symmetric modes dominate the spectra when the dipole induced dipole or bond polarizability are more important, respectively. This result explains why semiconductor nanoparticles with covalent bonds show intense symmetric scattering, and fluoride crystals with ionic bond show Raman scattering from quadrupolar modes, and why in oxide crystals the two modes show comparable Raman activity. A comparison of the spectra of titania, zirconia, and hafnia nanocrystals offers further support to the model.

Low-frequency Raman scattering is a widely used experimental technique for the study of the vibrational dynamics of metallic, semiconductor or dielectric nanoclusters, usually embedded in a glass.[1–9] Most theoretical approaches for the calculation of the acoustic vibrational dynamics of spheroidal clusters are based on the work of Lamb, which found the vibrations of a free homogeneous sphere.[10] The modes are classified in torsional and spheroidal, both labeled by three indices (lmn), which describe the angular (lm) and radial (n) dependence of the displacements. As shown by Duval on the basis of simple symmetry arguments, only the spheroidal symmetric $(l=0)$ and quadrupolar $(l=2)$ spheroidal modes are Raman active.[11] Furthermore, the $l=0$ modes give a polarized Raman spectrum, whereas the $l=2$ modes give depolarized spectra, allowing to distinguish the nature of the vibrations by a comparison of the VV and HV spectra. Recently, a paper appeared with the claim that the $l=0$ and $l=2$ spheroidal modes are not Raman active because of an odd displacement field.[12] This wrong criterium does not consider that even modes have usually odd displacements, as for example, the vibration of the oxygen molecule or the symmetric stretching of the CO_2 molecule, which are Raman active even modes, having odd displacements. In any case, the explicit calculation of the average strain starting from the potential, deriving the displacement and again deriving the strain components, shows that only the $l=0$ and $l=2$ spheroidal modes are Raman active.[13]

There are no general rules that indicate both the relative intensity of the symmetric and quadrupolar Raman peaks, appearing in the VV spectrum, or the depolarization ratio $DR_2=I_{HV}/I_{VV}$ for the quadrupolar modes. In fact, in some systems as silver, gold and PbF_2, the quadrupolar vibrations dominate the Raman spectrum, in other systems, as CdS, Si, Ga_2O_3, and HfO_2, the symmetric vibrations dominate.[3–6,8,9] In TiO_2 nanocrystals both modes are observed with similar intensities.[7] Different depolarization ratios for the quadrupo-

lar vibration have been measured, ranging from about 0.3 for silver to about 0.7 for TiO_2.[3,7]

In the case of metal particles, the resonance with the surface plasmon excitations produces intense low-frequency depolarized Raman scattering.[3,14,15] Here, we will limit our study to dielectric nanoparticles having electronic transition far from the excitation frequencies used in nonresonant Raman spectroscopy. The space-time changes of the polarization are usually separated in two contributes.[16] The first one is related to the density fluctuations, which cause inelastic neutron scattering and usually most of the VV Brillouin scattering, due to longitudinal acoustic phonons. The second contribution is due to changes of the dipole induced dipole (DID) effects, caused by the motion, and to changes of the bond polarizability (BP) with the change of the atomic distances. The induced effect contribute to the polarized Brillouin peak due to longitudinal phonons and cause the depolarized Brillouin peak, due to transversal phonons, and the disorder induced low-frequency Raman scattering in glasses or disordered crystals. The scattering mechanism in the low-frequency Raman scattering from the acoustic vibrations of nanoparticles is something in between to those of Raman and Brillouin scattering in bulk systems. If the particle is much smaller than the wavelength of the exciting light source, the mechanism of scattering due to density fluctuations is not active. All polarization elements are excited in phase and the particle behaves as a molecule, which can be described by an effective polarizability and by its derivatives with respect to the coordinates of the normal modes. However, the particle is sufficiently big to support acoustic modes with wavelengths much higher than the atomic sizes. Therefore, the effective polarizability tensor and the intensity of the Raman band of the active vibrations can be calculated with the method used for the calculation of the intensity of the Brillouin scattering. The important difference is that no q dependence is present, so that isotropic scattering is observed instead of the Bragg-

like scattering, typical of Brillouin scattering in systems, which extend over many wavelengths. A method for calculating the low-frequency Raman spectrum of dielectric nanoparticles has been developed in Ref. 13. The contribution of the pth mode to the Stokes part of the spectrum can be put in the form

$$I_{\alpha\beta}(\omega_p) \propto \frac{n(\omega_p)+1}{\omega_p} C_{\alpha\beta}(\omega_p), \tag{1}$$

where α and β are the directions of polarization of the incident and scattered photon, $n(\omega,T)$ is the Bose-Einstein factor, and $C_{\alpha\beta}(\omega_p)$ is the mode-radiation coupling coefficient. The scattering amplitudes of the pth mode $B^p_{\alpha\beta}=(C^p_{\alpha\beta})^{1/2}$ are given by

$$B^p_{\alpha\beta} = \sum_{\gamma\delta} \sum_i A_{\alpha\beta\gamma\delta}(\mathbf{x}^i) \frac{\partial e_\gamma(\mathbf{x}^i,p)}{\partial x_\delta}, \tag{2}$$

where $\mathbf{x}^i(t)$ is the equilibrium position of the ith scatterer, and the $\frac{\partial e_\gamma(\mathbf{x}^i,p)}{\partial x_\delta}$ are related to the strain components at $\mathbf{x}^i(t)$ produced by the normal mode $\mathbf{e}(i,p)$. The $A_{\alpha\beta\gamma\delta}$ coefficient are local quantities to be calculated at the equilibrium position of the ith unit and do not depend on the vibrations.

Within a DID model of the scattering mechanism, we will have

$$A_{\alpha\beta\gamma\delta}(\mathbf{x}^i) = \alpha_i \sum_j \alpha_i T_{\alpha\beta\gamma}(\mathbf{x}^{ij}) x^{ij}_\delta, \tag{3}$$

where α_i is the bare polarizability of the ith scatterer, $\mathbf{x}^{ij}=\mathbf{x}^j-\mathbf{x}^i$ is the equilibrium distance of the pair of scattering units i,j and $T^{(3)}_{\alpha\beta\gamma}(\mathbf{r})=-[\nabla_\alpha\nabla_\beta\nabla_\gamma(\frac{1}{|\mathbf{r}|})]$.

By neglecting the size dependence of the $A_{\alpha\beta\gamma\delta}$, i.e., by neglecting surface effects, and by converting the sum on the point scatterers into an integral on the volume of the sphere, in a continuum description of the vibrational modes, we finally obtain

$$B^p_{\alpha\beta} = N \sum_{k\gamma\delta} A^k_{\alpha\beta\gamma\delta} \int \frac{\partial e_\gamma(\mathbf{x},p)}{\partial x_\delta} dv, \tag{4}$$

where N is the number of unitary cells in the crystalline sphere and the sum over k is the sum over the atoms (ions) in the unit cell.

In this way, the problem of calculating the Raman intensities is reduced to the calculation of two set of independent quantities: (i) the $A_{\alpha\beta\gamma\delta}$, which are quantities that depend on the microscopic structure and on the scattering mechanism (DID or BP), but not on the dynamics; (ii) the average strain components produced by the vibrational mode, treated in a continuum approximation. The components of the local strain are calculated in the Lamb approximation of a homogeneous sphere, simply described by its density and isotropic transverse and longitudinal sound velocity.

The depolarization ratio DR_2 of the $l=2$ mode and the ratio of the coupling coefficients of the surface symmetric and quadrupolar modes $C_{02}=C_0/C_2$ have been calculated for some crystalline systems. A spherical cluster of radius R, centered on a particular atom is cut in the crystal. The quantities $A^k_{\alpha\beta\gamma\delta}$ are calculated in the different k sites by consid-
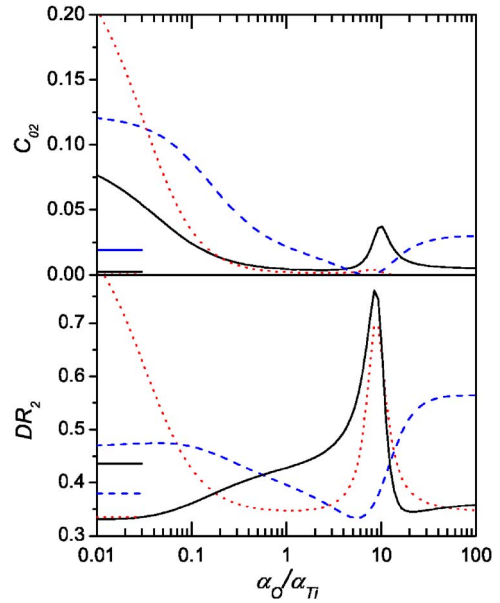
FIG. 1. (Color online) Calculated (DID model) DR_2 and C_{02} for TiO$_2$, as a function of the ratio of the polarizabilities of oxygen and titanium ions. Full line: brookite, dotted line: anatase, dashed line: rutile. The horizontal segments to the left give the quantities calculated in a NNDID model.

ering the induced fields from a sufficient number of shells around the kth site. In particular, the contribution of the first shell of nearest neighbor atoms is calculated.

The structure of the $A_{\alpha\beta\gamma\delta}$ in a cubic Bravais lattice and of the strain tensor $\varepsilon_{\alpha\beta}$ for the $l=0$ makes $C_0=0$ and $DR_2 =1/3$.[13] These two results can be extended to simple cubic system, as diamond, NaCl, CsI, PbF$_2$, in which all atoms in the unitary cell have cubic site symmetry. This is because the scattered field is the sum of the fields scattered by each atom.

In noncubic systems, DR_2 and C_{02} depend on the atomic polarizabilities. In binary systems, a single parameter, the ratio of atomic polarizabilities of the two atomic species, is needed. Figure 1 shows the calculated DR_2 and C_{02} for the three TiO$_2$ structures, tetragonal rutile, tetragonal anatase, and monoclinic brookite, as a function of the atomic polarizability ratio.

The DR_2 curve of anatase shows that the Ti-Ti DID effects (left side of the figure) are strongly depolarized, that the O-O contribution (right side) have low depolarization ratio and that the combined effects of O-O, Ti-Ti, and O-Ti produce a critical DR_2 behavior caused by the interference of the induced fields. In the case of rutile, for a polarizability ratio $\alpha_{O^{2-}}/\alpha_{Ti^{4+}} \simeq 8$ these interference effects simulate a cubic symmetry with $DR_2=1/3$ and $C_{02}=0$. A pronounced maximum of DR_2 is found at $\alpha_{O^{2-}}/\alpha_{Ti^{4+}} \simeq 8$ for the anatase and brookite structure. The polarizabilities are not well defined quantities that can be assigned to a given ion, independent on the context and different values, covering wide ranges, can be found in the literature. A possible criterion is to estimate a value of the polarizability proportional to the atomic volume.[17] Another criterion is to measure the atomic distances and the dielectric constant of different compounds assigning an effective radius and polarizability to each atom
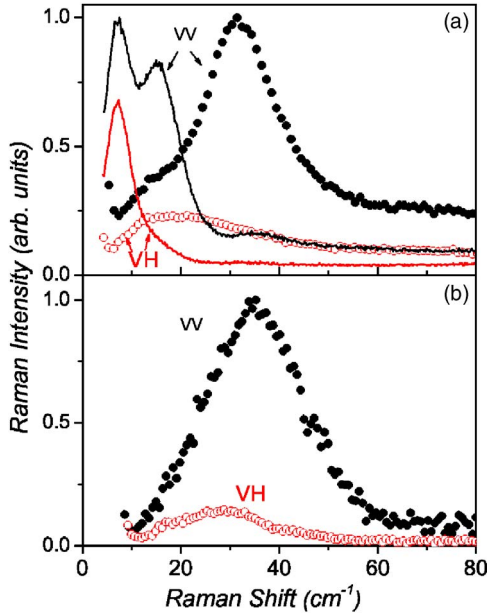
FIG. 2. (Color online) VV and VH polarized Raman spectra of (a) (full lines) silica-titania (with TiO$_2$ nanoparticles [7]) and (circles) silica-hafnia (with HfO$_2$ nanoparticles [5]); (b) silica-zirconia (with ZrO$_2$ nanoparticles).

TABLE I. Depolarization ratio of the $l=2$ mode and ratio of the coupling coefficients of the $l=0$ and $l=2$ modes.

System	DR$_2$	C$_{02}$	Ref.
PbF$_2$	0.5±0.1	1.0±0.4	6
TiO$_2$	0.7±0.1	7±2	7
Ga$_2$O$_3$		12±4	4
CdS-CdSe		>20	9
HfO$_2$	0.8±0.2	30±8	5
ZrO$_2$		>20	present

or ion.[18] The two methods give different results, especially when the bonds have mixed ionic and covalent nature and the ionic charge is not well defined. In the case of O^{2-}, the two methods give an ionic radius of 55 and 138 pm, respectively (44 and 57 pm for Ti^{4+}), from which values of 1.9 and 14 for the $\alpha_{O^{2-}}/\alpha_{Ti^{4+}}$ ratio can be estimated. From the spectra of Fig. 2(a) for silica-titania glassceramics, DR$_2$=0.7±0.1 is obtained. This value can be reproduced only in the small range of the resonance at $\alpha_{O^{2-}}/\alpha_{Ti^{4+}} \simeq 9$ in Fig. 1, the maximum value being just DR$_2$=0.7.

The peak intensities of the $l=0$ and $l=2$ surface vibrations are comparable in the VV spectrum of Fig 2(a) for TiO$_2$. From the spectra a value of $C_{02}=7±2$ is obtained. It should be noted that the ratio of the peak intensities in the Raman spectrum is reduced, with respect to the C_{02} ratio, by a factor of the order of $(\omega_0/\omega_2)^3$, because of the $(n+1)/\omega \simeq \omega^2$ factor [see Eq. (1)] and because of a peak broadening due to a size distribution with $\Delta\omega_0/\omega_0 \simeq \Delta\omega_2/\omega_2$.

The calculations were performed for many other systems of interest, as quartz, christobalite, Ga$_2$O$_3$, HfO$_2$. In some cases the dependence of DR$_2$ on the ratio of ionic polarizabilities is not so critical as for TiO$_2$ crystals. A common result of all investigated systems is that $C_{02} \ll 1$. This is related to the intrinsically depolarized nature of the DID effect, but also to the fact that at the microscopic scale of the first neighbor atoms, high symmetry is present even in lattices with low symmetry. For this reason, the deviation from the simple structure of the cubic $A^k_{\alpha\beta\gamma\delta}$ is not really very important.

Therefore, we need other scattering mechanisms, different from DID, for accounting for the observation of intense peaks from the symmetric mode in the Raman spectra of many systems. A bond polarizability mechanism is often taken into account by considering the DID effect limited to

the nearest neighbors atoms (NNDID).[19] The results of this calculation are reported in Fig. 1 as horizontal segments, since DR$_2$ and C_{02} do not depend on the ratio of polarizabilities. The intensity of the symmetric mode remains very weak also in the NNDID model.

However, the NNDID model does not fully reproduce the BP mechanism. When atoms move, bonds also move, producing fluctuations of the induced fields, and this effect is accounted for by NNDID. But bond stretching, by changing the charge distribution within the volume of the covalent bond, will also change the value of the bond polarizability. In general, different effects will be present for fields parallel or perpendicular to the bond direction $\alpha_\parallel$ and $\alpha_\perp$. We are interested to the derivatives of the polarizability with respect to bond length and we can define an isotropic $\alpha'=1/3$ ($\alpha'_\parallel +2\alpha'_\perp$) and an anisotropic $\gamma'=\alpha'_\parallel - \alpha'_\perp$ derivative.

The isotropic term has $A_{\alpha\beta\gamma\delta}=A\ \delta_{\alpha\beta}\delta_{\gamma\delta}$. By using the relations among the strain components in Table I of Ref. 13, one obtains that α' produces Raman scattering from the symmetric modes, but not from the quadrupolar modes. From a more physical point of view, we can observe that most bonds are stretched in phase in a surface symmetric mode, producing a modulation of the total polarizability of the sphere. On the contrary, for the quadrupolar modes, the total polarizability of the sphere does not change in time because the bonds are stretched with phase relations that maintain the average bond length constant.

The anisotropic term γ' will contribute to depolarized scattering and indeed to the Raman activity of the quadrupolar mode. Its importance will depend on the γ'/α' ratio, but also on the crystal structure with its distribution of bond directions. It should be noted that when the polarization of the exciting light is parallel or perpendicular to the bond direction, no depolarized scattering will occur. Furthermore, depolarized fields produced by bonds with different orientation will sum up with a tendency to destructive interference. For these reasons, within a bond polarizability scattering mechanism, it is expected that the Raman activity of the quadrupolar vibrations is much smaller than that of the symmetric ones.

The above analysis seems to bring forward a quite simple result. The relative importance of the symmetric and quadrupolar modes in the Raman spectra is mainly related to the scattering mechanism, BP or DID. The few available experimental data are reported in Table I, where the systems are ordered in increasing C_{02} values. PbF$_2$ has the smallest C_{02}

value in agreement with a high ionic character of the bonds. The $DR_2 = 0.5 \pm 0.1$ is higher than the calculated one for a cubic system ($DR_2 = 0.33$), but this could be due to the fact that the investigated nanocrystals were highly defective, due to a high Er^{3+} doping. On the low side of Table I we find CdS_xSe_{1-x}, indicating that the BP mechanism of scattering dominates in covalent systems. In between we find Ga_2O_3 and TiO_2, which are systems where the ionic and covalent nature of the bonds compete.

Tetragonal HfO_2 has a quite strong scattering from the symmetric modes.[5] Silica-zirconia glassceramics were produced for a comparison with the titania and hafnia systems. The waveguides fabricated by dip coating with compositions $80SiO_2 - 20ZrO_2$ were annealed at different temperatures ($900\ °C < T < 1300\ °C$) for promoting the growth of ZrO_2 nanocrystals of increasing size. The polarized Raman spectra of these systems, obtained by waveguide excitation in the TE_0 mode, are shown in Fig. 2(b) for the waveguide annealed at $1150\ °C$. The spectra of zirconia and hafnia nanocrystals look very similar with dominant scattering from the $l = 0$ vibrations, whereas anatase has also an important scattering from the $l = 2$ modes. A common trend would be expected for the three oxides with bonds involving $3d$, $4d$, and

$5d$ electrons, respectively. However, hafnia and zirconia have very similar structures and absorption edges, quite different from those of anatase.[20] This suggests that also the nature of the bonds are different. A quantitative comparison of the three systems would need first principle calculation of the polarizabilities, and their derivatives with the strain.

In conclusion, we have found that DID scattering mechanism produce depolarized Raman spectra and indeed Raman scattering from the quadrupolar vibrations. DR_2 depends on the crystalline structure and on the ratios of polarizabilities of the different dipoles. The symmetric mode is forbidden in cubic systems and has whatever quite low intensity in all systems. BP scattering mechanism mainly gives polarized Raman spectra and indeed Raman from the symmetric vibrations. A correlation seems to exist between the C_{02} and the degree of ionicity/covalency nature of the bonds. Accurate measurements of DR_2 and C_{02} in many systems are now needed to test this model.

*Email address: mattarel@science.unitn.it

[1] E. Duval, A. Boukenter, and B. Champagnon, Phys. Rev. Lett. **56**, 2052 (1986).

[2] G. Mariotto, M. Montagna, G. Viliani, E. Duval, S. Lefrant, E. Rzepka, and C. Mai, Europhys. Lett. **6**, 239 (1988).

[3] M. Fujii, T. Nagareda, S. Hayashi, and K. Yamamoto, Phys. Rev. B **44**, 6243 (1991).

[4] R. Ceccato, R. Dal Maschio, S. Gialanella, G. Mariotto, M. Montagna, F. Rossi, M. Ferrari, K. E. Lipinska-Kalita, and Y. Ohki, J. Appl. Phys. **90**, 2522 (2001).

[5] Y. Jestin, N. Afify, C. Armellini, S. Berneschi, S. N. B. Bhaktha, B. Boulard, A. Chiappini, A. Chiasera, G. Dalba, C. Duverger, M. Ferrari, C. E. Goyes Lopez, M. Mattarelli, M. Montagna, E. Moser, G. Nunzi Conti, S. Pelli, G. C. Righini, and F. Rocca, Proc. SPIE **6183**, 438 (2006).

[6] V. K. Tikhomirov, D. Furniss, A. B. Seddon, M. Ferrari, and R. Rolli, Appl. Phys. Lett. **81**, 1937 (2002).

[7] M. Montagna, E. Moser, F. Visintainer, L. Zampedri, M. Ferrari, A. Martucci, M. Guglielmi, and M. Ivanda, J. Sol-Gel Sci. Technol. **26**, 241 (2003).

[8] M. Ivanda, A. Hohl, M. Montagna, G. Mariotto, M. Ferrari, Z. Crnjak Orel, A. Turkovic, and K. Furic, J. Raman Spectrosc. **37**, 161 (2006).

[9] M. Ivanda, K. Babosci, C. Dem, M. Schmitt, M. Montagna, and W. Kiefer, Phys. Rev. B **67**, 235329 (2003).

[10] H. Lamb, Proc. London Math. Soc. **13**, 187 (1882).

[11] E. Duval, Phys. Rev. B **46**, 5795 (1992).

[12] M. Kanehisa, Phys. Rev. B **72**, 241405(R) (2005).

[13] M. Montagna and R. Dusi, Phys. Rev. B **52**, 10080 (1995).

[14] B. Palpant, H. Portales, L. Saviot, J. Lerme, B. Prevel, M. Pellarin, E. Duval, A. Perez, and M. Broyer, Phys. Rev. B **60**, 17107 (1999).

[15] G. Bachelier and A. Mlayah, Phys. Rev. B **69**, 205408 (2004).

[16] P. Benassi, O. Pilla, V. Mazzacurati, M. Montagna, G. Ruocco, and G. Signorelli, Phys. Rev. B **44**, 11734 (1991).

[17] D. C. Ghosh and R. Biswas, Int. J. Mol. Sci. **4**, 379 (2003).

[18] R. D. Shanon and C. T. Prewitt, Acta Crystallogr., Sect. A: Cryst. Phys., Diffr., Theor. Gen. Crystallogr. **32**, 751 (1976).

[19] V. Mazzacurati, M. Montagna, O. Pilla, G. Viliani, G. Ruocco, and G. Signorelli, Phys. Rev. B **45**, 2126 (1992).

[20] M. Mero, J. Liu, W. Rudolph, D. Ristau, and K. Starke, Phys. Rev. B **71**, 115109 (2005).